Structural Engineering and Mechanics, *Vol. 60, No. 2 (2016) 225-235*
DOI: http://dx.doi.org/10.12989/sem.2016.60.2.225

Polypropylene fiber reinforced concrete plates under fluid impact. Part II: modeling and simulation

Hasan Korucu*[1,2]

[1]*Turkish Armed Forces Headquarters, Department of Engineering, 06100 Bakanliklar, Ankara, Turkey*
[2]*Purdue University, Lyles School of Civil Engineering, West Lafayette, IN 47907, United States*

(Received March 29, 2016, Revised June 15, 2016, Accepted June 16, 2016)

Abstract. Fluid impact tests on plates containing mesh reinforcement and polypropylene fibers were modeled and simulated using explicit finite element analysis software, LS-DYNA. The scabbing dimensions obtained by the experiments and the simulations were compared and crack formations were matched. The objective was to test the accuracy and fidelity of the model and to confirm that damage caused by fluid impact on the plates can be estimated with a reasonable accuracy over a wide range of impact velocity.

Keywords: fluid impact; polypropylene fibers; projectile; LS-DYNA; smoothed particle hydrodynamics

1. Introduction

In the companion to this paper, high velocity fluid impact experiments on reinforced concrete plates consisting various amounts of polypropylene fibers were presented. Water-filled cylindrical aluminum cans were launched at the specimens at 70 to 207 m/s velocity range. Impact velocities were captured using a high-speed camera and laser beams. Static tests were also performed to identical specimens to define static failure mode. The material tests which carried out to identify the material parameters were also described.

Taking a brief look at literature, numerous studies can be found on modeling concrete structures subjected to several types of impact loading. Micheli *et al*. (2015) used a damage model in simulating the collision of hard steel spheres against aluminum thin circular plates at speeds up to 140 m/s by finite element analysis employing axisymmetric, shell and solid elements with various parameters of the numerical analysis. Thai and Kim (2015) presented numerical analysis of reinforced concrete slabs under missile impact loading which was modeled using LS-DYNA where material nonlinearity considering damage was included in the analysis. Gülkan and Korucu (2011) simulated high-velocity impact of large caliber tungsten projectile on concrete composite plates by ABAQUS modeling with a damaged plasticity model for concrete. Pandey (2010) carried out a comparative study of non-linear response of reinforced concrete nuclear containment cylindrical shell subjected to impact of an aircraft and explosion of different amounts of blast charges and implemented a material model which takes the strain rate sensitivity in dynamic

∗Corresponding author, Ph.D., E-mail: korucu_h@yahoo.com

http://www.techno-press.org/?journal=sem&subpage=8 ISSN: 1225-4568 (Print), 1598-6217 (Online)

loading situations, plastic and visco-plastic behavior in three dimensional stress state and cracking in tension into account into a finite element code.

Riera (1968) proposed a perfectly plastic impact model without taking the elastic behavior of the projectile into account for a thin-walled cylinder representing a high velocity impact of an aircraft onto a nuclear reactor. Sugano *et al*. (1993) defined a discrete model expressing the elastic behavior of an aircraft based on Newmark-β method.

Methods for modeling the water were developed by researchers. A mesh-free Lagrangian method, Smoothed Particle Hydrodynamics (SPH), used in general to represent fluids, was developed by Lucy (1977), Gingold and Monaghan (1977) and used introducing material strength by Libersky and Petschek (1991). Anderson *et al*. (1999), who created a model based on Eulerian wavecode CTH for the impact of a projectile into a water-filled tank. An Arbitrary Lagrangian-Eulerian (ALE) and an SPH approach was compared by Varas *et al*. (2009) to indicate the extrication of the fluid in the simulation of impact on an airplane wing tank model using LS-DYNA. Vignjevicz *et al*. (2002) and Maurel *et al*. (2009) also used SPH in modeling fluid in their studies and obtained satisfying results. The nonlinear numerical analysis of the impact response of reinforced concrete/mortar beam incorporated with the SPH by Mokhatar *et al*. (2015) where three material models were used to express the complex behavior of concrete material during short time loading condition.

In this study, modeling and simulation of experiments stated in Korucu (201X) were presented. The scabbing dimensions obtained by the experiments and the simulations were compared and crack formations were matched visually. LS-DYNA, explicit finite element analysis software, was used to simulate the response of the specimens to fluid impact (LS-DYNA 2005). Experimental results were used to test the accuracy and fidelity of the model. The impact velocity of the fluid-filled cans was the independent variable. Visual similarity and the scabbing formation in the experimental and computational specimens' post-impact state were used as measures of goodness of computational model. It was aimed to confirm that damage caused by fluid impact on the reinforced concrete plates can be estimated with reasonable accuracy over a wide range of impact velocity.

2. Numerical analysis and simulations

LS-DYNA v.9.71 software was used to model the projectile and target spectrum and to simulate the impact tests and to analyze the impact resistance of the plates. The aim of these simulations was to test the accuracy and fidelity of the numerical modeling approach.

Concrete and support plates were modeled with solid elements, while reinforcing bars were modeled with beam elements in the construction of the computational model. Aluminum can was modeled with shell elements and water was modeled with SPH. Contact between water and thin-walled aluminum can and between water and concrete was defined by "automatic nodes-to-surface" algorithm. "Automatic surface-to-surface" algorithm was used to define the contact between aluminum can, concrete and support plates. *CONSTRAINED_LAGRANGE_IN_SOLID which provides the coupling mechanism for modeling fluid-structure interaction was used to define the bond between the concrete and the reinforcement bars. The structure was constructed from Lagrangian shell and/or solid entities. The aluminum can including fluid body was set into motion with *INITIAL_VELOCITY_GENERATION command which is used to define velocities for rotating and translating bodies (LS-DYNA 2003). Figs. 1-2 show the modeling details of the

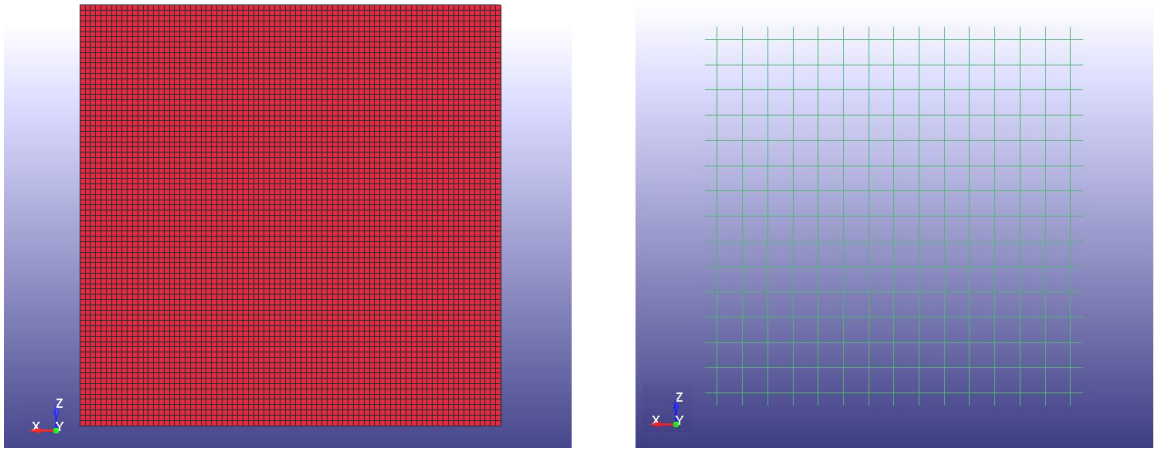

(a) Plate (b) Reinforcement Bars

Fig. 1 Modeling

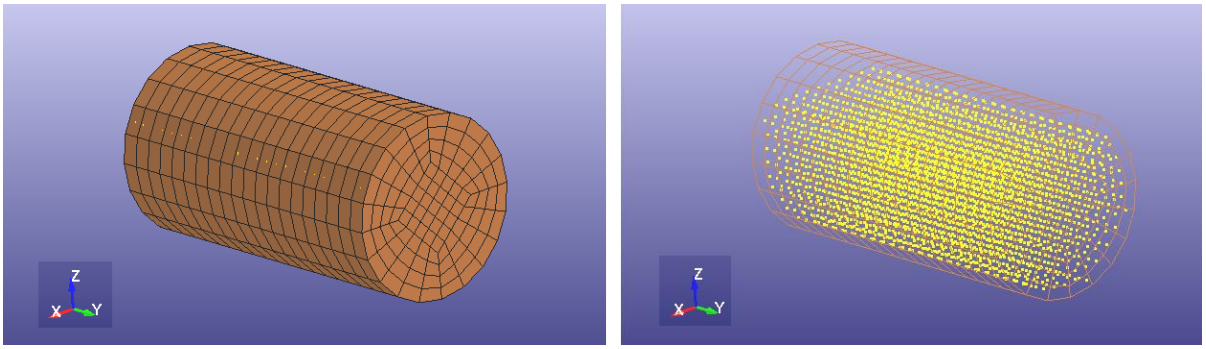

(a) Cylindrical can (b) Water

Fig. 2 Modeling

members. Computational set up and simulation at the time of impact was shown in Figs. 3-4.

The solid member representing plates was restrained along the top and bottom edges against rotation and displacement at all directions, but unrestrained for vertical displacement at the upper support as in the experiments. The steel plates used as supports were restrained against both displacement and rotation in all directions.

LS-DYNA Material Type 84 (*MAT_WINFRITH_CONCRETE) which includes rate effects was used in modeling the concrete. The Winfrith concrete model, defined as a smeared crack or pseudo crack model, was developed by Broadhouse and Neilson (1987), and Broadhouse (1995). The plasticity portion of the model was based upon the shear failure surface proposed by Ottosen (1977).

$$F(I_1, J_2, \cos 3\theta) = a\frac{J_2}{(f_c')} + \lambda\frac{\sqrt{J_2}}{f_c'} + b\frac{I_1}{f_c'} - 1 \tag{1}$$

where a and b are the constants controlling the meridional shape of the shear failure surface, $\lambda = \lambda(\cos 3\theta)$ ranging $-1 \leq \cos 3\theta \leq +1$ for triaxial compression to triaxial extension control

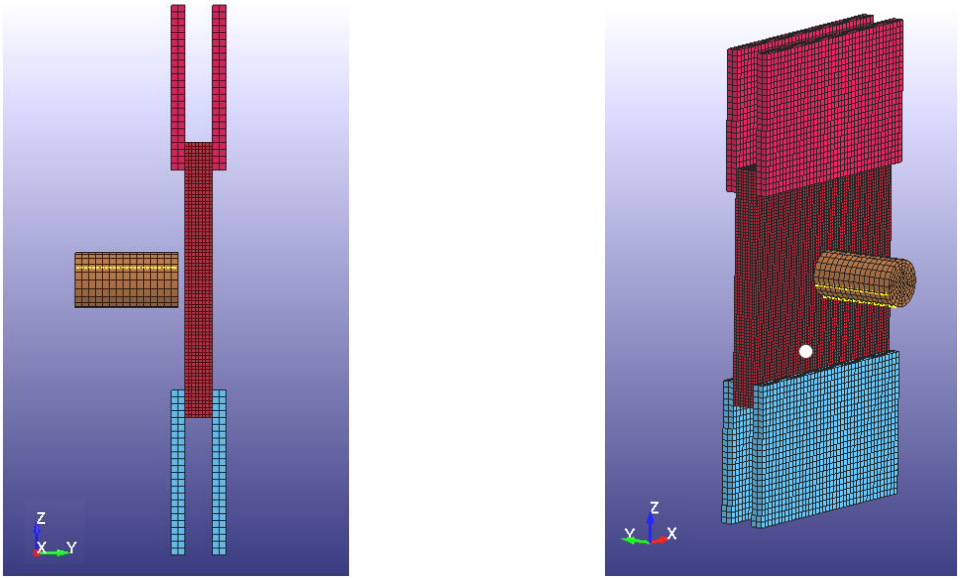

(a) Side-view (b) Isometric view

Fig. 3 Computational setup

the shape of the shear failure surface on the π-plane, $f_c'$is unconfined compressive strength, and the independent parameters $I_1$and J_2 are the invariants of the stress tensor. Rate effects were taken into account with the formulation of CEB (1988) which the strain rate enhancements are based upon incremental rates

$$\dot{\varepsilon}_{ij} = \frac{\Delta\varepsilon_{ij}^{n}}{\Delta t} \tag{2}$$

where $\Delta\varepsilon_{ij}^{n}$ is the current strain rate increment, Δt is the current time step and $\dot{\varepsilon}$ is the incremental effective strain rate.

Steel for reinforcing bars and aluminum for the can were defined by LS-DYNA Material Type 3 (*MAT_PLASTIC_KINEMATIC). The model, which was suitable to introduce isotropic and kinematic hardening plasticity including rate effects, was very effective and available for beam, shell and solid elements (LS-DYNA 2003). Rate effects taken into account were formulated by Malvar (1998).

Water was modeled using with LS-DYNA Material Type 9 (*MAT_NULL) which allows defining viscosity and equations of state to be considered without computing deviatoric stresses (LS-DYNA 2003).

The material parameters used in the LS-DYNA analysis are given in Tables 1-4 where σ and τ are compressive and tensile strengths, respectively.

Plastic strain was the basis for failure criteria for steel bars and aluminum so that when plastic strain was exceeded, element was assumed failed and eliminated from the model. Assumed plastic limits for steel and aluminum were 30% and 20%, respectively. For concrete, erosion was defined to take effect when the maximum strain exceeded 10%. The run-time of each simulation was approximately 3 to 6 hours on a community cluster consisting of 8 CPUs.

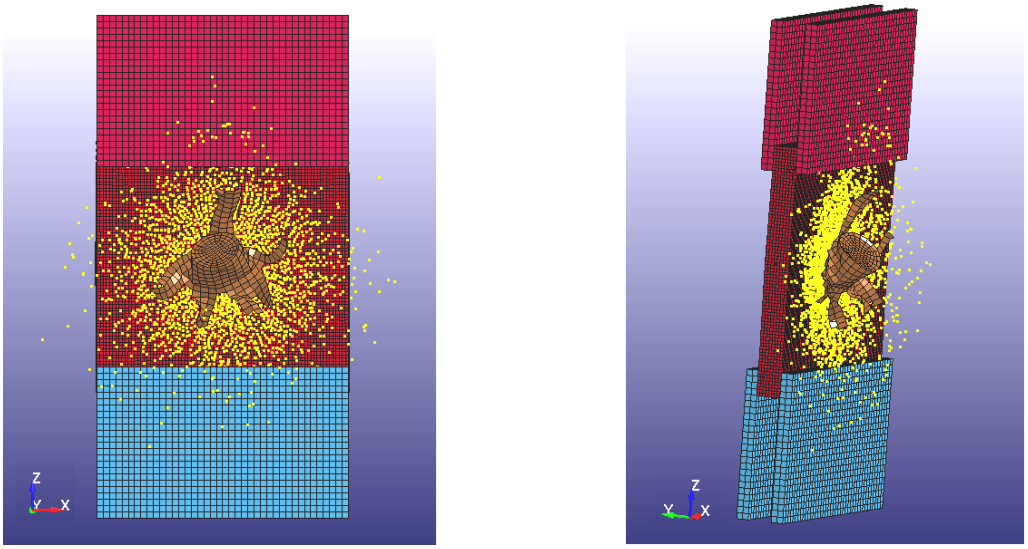

(a) Side-view (b) Isometric view

Fig. 4 Computational setup

Table 1 Mechanical properties of concrete

Group No.	σ_c (MPa)	τ_c (MPa)	E_c (GPa)	ϑ_c	ρ_c (kg/m^3)
1	33.26	1.89	23.40	0.15	2500
2	35.56	4.19	23.40	0.15	2500
3	35.43	4.72	23.40	0.15	2500
4	34.65	5.12	23.40	0.15	2500

Table 2 Mechanical properties of ϕ16 wire

f_y^s (MPa)	E_s (GPa)	ϑ_s	ρ_s (kg/m^3)
275.79	200	0.30	7850

Table 3 Mechanical properties of aluminum

f_y^a (MPa)	E_a (GPa)	ϑ_a	ρ_a (kg/m^3)
275	69	0.30	2750

Table 4 Mechanical properties of water

μ_w (Ns/m^3)	ρ_w (kg/m^3)
10^{-3}	1000

3. Results and discussions

The deformed experimental specimens and those simulated for impact are compared visually in Figs. 5-6. Pictures show that there is good agreement between the failure types and deformed

shapes in most of the specimens. In the computational simulations, material parameters were calibrated to match the experimental observation. Compressive and tensile strength of concrete were determined by performing material tests. The ϕ16 wire could not be subjected to tensile test because of its small cross-section, which had a diameter of 1.6 mm. Instead, material properties of wire provided in manufacturer catalogs were used. The most remarkable mismatch between experimental and calculated results may arise partly from shortcomings of defining material characteristics. Nonetheless, acceptable results were obtained as presented in the Figs. 5-6.

Scabbing dimensions on the rear sides were obtained experimentally and numerically and these values are compared in Table 5.

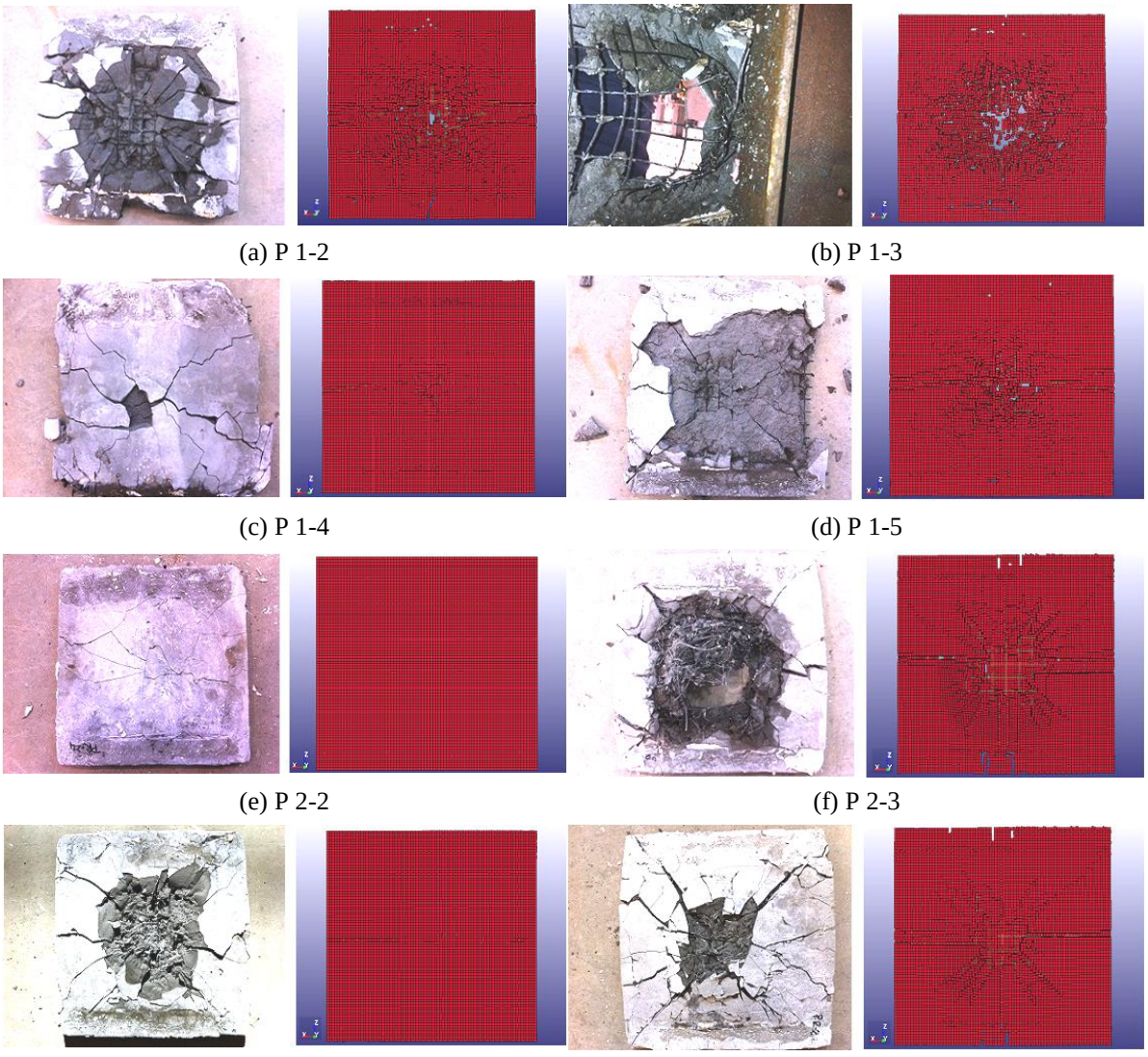

(a) P 1-2 (b) P 1-3

(c) P 1-4 (d) P 1-5

(e) P 2-2 (f) P 2-3

(g) P 2-4 (h) P 2-5

Fig. 5 Comparison of experimental and analytical results of specimens (rear sides)

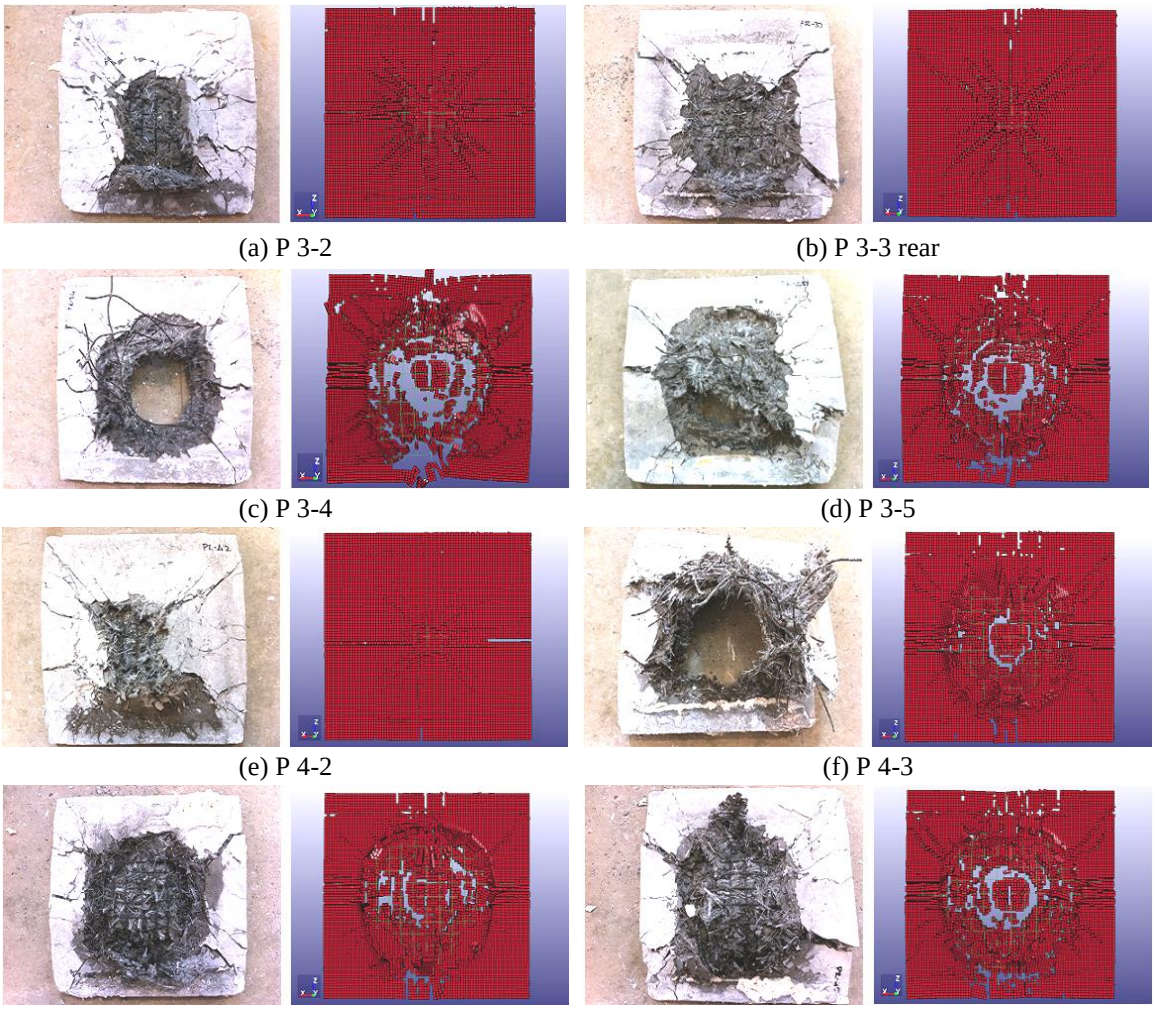

(a) P 3-2 (b) P 3-3 rear

(c) P 3-4 (d) P 3-5

(e) P 4-2 (f) P 4-3

(g) P 4-4 (h) P 4-5

Fig. 6 Comparison of experimental and analytical results of specimens (rear sides)

Investigating the results of the experiments and the simulations, a reasonable match in scabbing dimensions can be seen. Crack formations are visually compatible. Table 6 shows a summary of comparison for scabbing dimensions observed both experimentally and analytically. Models showed acceptable and compatible results with the specimens with error ratios between 1 % and 11% except for a remarkable result of 42% error in vertical direction for specimen P 4-2. Even so, both specimen P 4-2 and the model showed scabbing, not total failure. Table 6 shows that fibers helped to avoid total disintegration and the size of the scabbed area on the rear face decreased with the increase in fiber ratio.

Figs. 7-8 shows the scabbing dimensions variation by amount of fiber for specimens P 1-3, P 2-3, P 3-2 and P 4-2 which have impact velocities of 132, 136, 136 and 125 m/s, respectively. The graph was formed to observe the effect of fiber amount on the resistance of specimens that were impacted at similar velocities. Increase in the amount of fiber causes reduction in the dimension of

Table 5 Comparison of scabbing dimensions at rear face

No	Impact Velocity (m/s)	Scabbing Dimensions (mm)				Error (%)	
		Experimental		Numerical		Horz.	Vert.
		Horz.	Vert.	Horz.	Vert.		
P 1-2	101	122	163	115	158	6	3
P 1-3	132	142	78	155	81	9	4
P 1-4	74	N/A	N/A	N/A	N/A	N/A	N/A
P 1-5	94	146	162	138	149	5	8
P 2-2	70	N/A	N/A	N/A	N/A	N/A	N/A
P 2-3	136	146	158	152	165	4	4
P 2-4	97	123	126	N/A	N/A	N/A	N/A
P 2-5	130	81	78	76	71	6	9
P 3-2	136	96	114	91	105	5	8
P 3-3	167	146	148	154	158	5	7
P 3-4	207	161	164	156	159	3	3
P 3-5	190	148	163	155	168	5	3
P 4-2	125	71	98	63	57	11	42
P 4-3	163	157	159	156	165	1	4
P 4-4	161	149	167	158	176	6	5
P 4-5	183	141	149	155	142	10	5

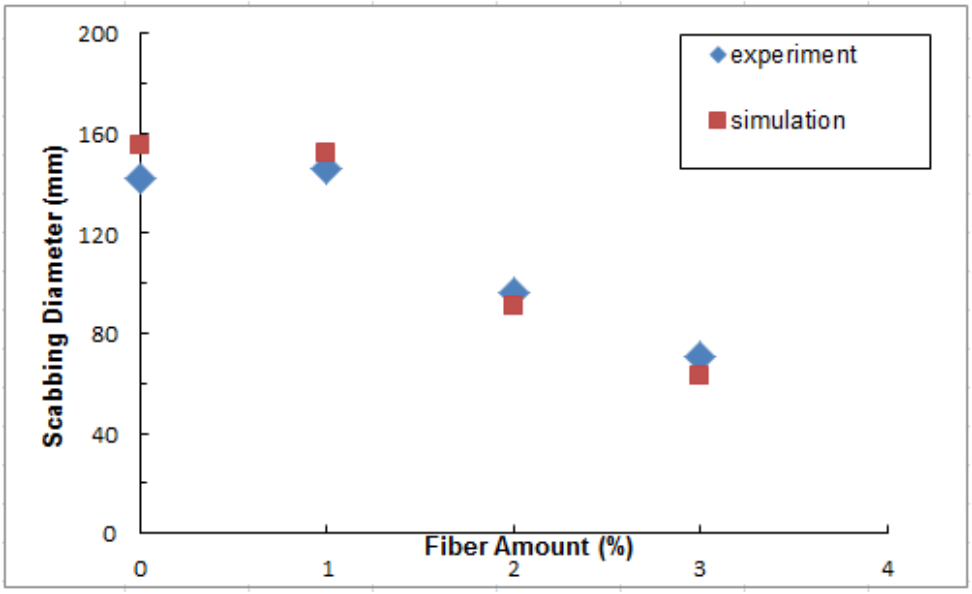

Fig. 7 Scabbing dimensions (rear face-horizontal) distribution by fiber amount

scabbing. This behavior may be seen with good agreement between experimental and numerical results in Fig. 7 in horizontal direction. In the vertical direction, in Fig. 8, specimen P 1-3 that was

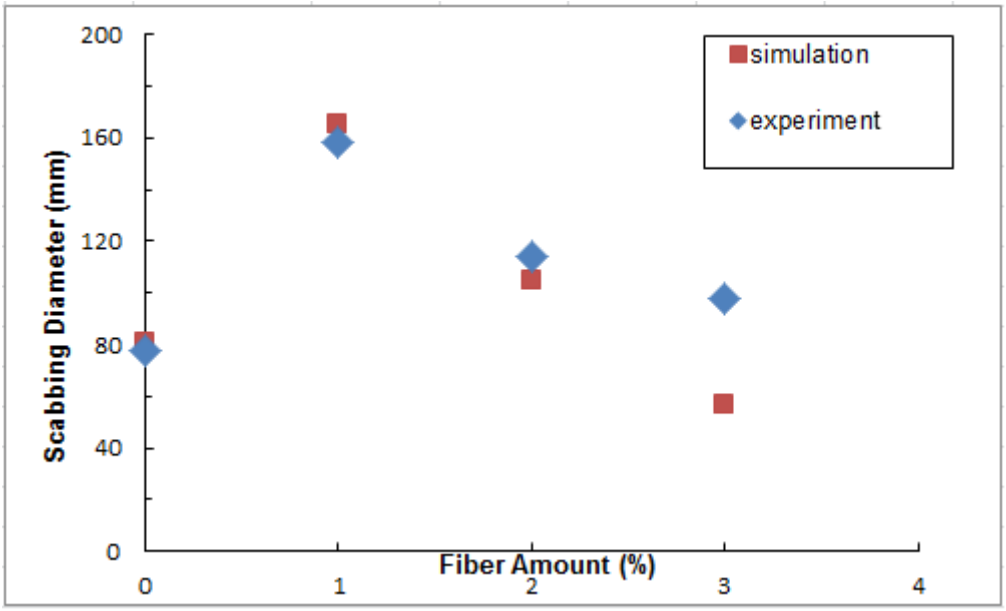

Fig. 8 Scabbing dimensions (rear face-vertical) distribution by fiber amount

not fabricated with fibers had smaller scabbing dimension. This value does not reflect the actual behavior as total disintegration occurred and disintegrated concrete pieces stayed on the reinforcement did not have strength or any capacity left.

Reduction in the compressive strength, which was the critical parameter in resisting impact, was identified in material tests. Albeit fibers increased the strength against fluid impact, the main member contributing to resistance was the reinforcement bars. Results from experiments on SIFCON specimens produced only with polypropylene fibers and cement slurry exhibited outcomes supporting this observation (Korucu 2012).

4. Conclusions

In this paper, laboratory fluid impact experiments presented in Part I of this study were simulated and the accuracy of the simulation software and the fidelity of the computational model were tested (Korucu 2016). The primary objective of the study was to observe the resistance of concrete plates with various amounts of polypropylene fibers against fluid impact. The projectile was a thin-walled aluminum can filled with water with an average weight of 185 g. The impact velocity varied between 70 and 207 m/s. The targets were 254×254×25.4 mm concrete plates. All plate types were tested statically to determine flexural capacity and failure type**.** All of the experiments were recorded by a high-speed camera. Impact velocities were determined using both high-speed camera and laser beams. The scabbing dimensions were measured after impact tests.

The numerical results revealed that the non-linear softening behavior of reinforced concrete plates with various amounts of polypropylene fibers can be incorporated in the proposed material model.

Fibers helped to avoid total disintegration and the size of the scabbed area on the rear face

decreased with the increase in fiber ratio. This behavior was also observed in the simulation results.

Estimates based on computational simulations agreed with experimental results regarding crack pattern and extent of scabbing damage, when occurred, mismatch between experimental and calculated results may arise partly from shortcomings of defining material characteristics.

LS-DYNA, the computational simulation platform, gave acceptable results in the estimation of deformation profile and failure types. Winfrith concrete model was used for concrete. The error percentages remained mostly at low levels for the deflection values. Given the idealizations of the physical conditions, observed differences between experimental tests and numerical simulations were not unexpected.

Acknowledgements

The author acknowledges Prof. Mete A. Sozen and Assoc.Prof. Ayhan Irfanoglu for their supervision during period of the study, and Dr. Efe Kurt, Dr. Oscar Alfredo Ardila-Giraldo and Dr. Seyed Hamid Changiz Rezaei for their help and contributions to the work.

This research was made possible by the support from the Scientific and Technological Research Council of Turkey (TUBITAK) for the author in the form of a post-doctoral scholarship at Purdue University.

References

Anderson, C.E., Sharron, T.R., Walker, J.D. and Freitas, C.J. (1999), "Simulation and analysis of a 23-mm HEI projectile hydrodynamic ram experiment", *Int. J. Impact Eng.*, **22**(9-10), 981-997.

Broadhouse, B.J. (1995), "The Winfrith concrete model in LS-DYNA3D", Report No.: SPD/D (95)363, Structural Performance Department, AEA Technology, Winfrith Technology Centre Dorchester, UK.

Broadhouse, B.J. and Neilson, A.J. (1987), "Modelling reinforced concrete structures in DYNA3D", *Paper Presented at DYNA3D User Group Conference, Safety and Engineering Science Division, United Kingdom Atomic Energy Authority, Winfrith, AEEW-M 2465*, London, October.

CEB (1988), "Concrete structures under impact and impulsive loading", Synthesis Report, Bulletin Number: 187, Comite Euro-International du Beton, Dubrovnik, Croatia.

Gingold, R.A. and Monaghan, J.J. (1977), "Smoothed particle hydrodynamics: Theory and application to nonspherical stars", *Mon. Not. R. Astron. Soc.*, **181**, 375-389.

Gülkan, P. and Korucu, H. (2011), "High-velocity impact of large caliber tungsten projectiles on ordinary Portland and calcium aluminate cement based HPSFRC and SIFCON slabs. Part II: numerical simulation and validation", *Struct Eng Mech*, **40**(5), 617-636.

Korucu, H. (2012), "Askeri binalarin ve stratejik sivil yapilarin patlama ve darbeye dayanikli olarak tasarlanmasina yönelik bütünleyici bir araştirma: Laboratuar deneyleri, doğrulayici ve büyük ölçekli simülasyonlar ve mühendislik tasarim prensipleri", Final Report: Post-Doctoral Research Scholarship Number 2219, Scientific and Technological Research Council of Turkey (TUBITAK), Ankara, Turkey.

Korucu, H. (2016), "Polypropylene fiber reinforced concrete plates under fluid impact. Part I: experiments", *Struct Eng Mech*, **60**(2), 211-223.

Libersky, L.D. and Petschek, A.G. (1991), "Smooth particle hydrodynamics with strength of materials", *Proceedings of the Next Free-Lagrange Method*, Eds. Trease, H.E., Fritts, M.J., Crowley, W.P., Lecture Notes in Physics, Vol. 395, Springer, Berlin.

LS-DYNA (2003), Keyword User's Manual Version 970, Livermore Software Technology Corporation

(LSTC), Livermore, CA, USA.
LS-DYNA (2005), v970 r5434a SMP Version, Livermore Software Technology Corporation (LSTC), Livermore, CA, USA.
Lucy, L.B. (1977), "A numerical approach to the testing of the fission hypothesis", *Astron. J.*, **82**, 1013-1024.
Malvar, L.J. (1998), "Review of static and dynamic properties of steel reinforcing bars", *ACI Mater. J.*, **95**(5), 609-616.
Maurel, B., Potapoc, S., Fabis, J. and Combescure, A. (2009), "Full SPH fluid-shell interaction for leakage simulation in explicit dynamics", *Int. J. Numer. Meth. Eng.*, **80**(1), 210-234.
Micheli, G.B., Driemeier, L. and Alves, M. (2015), "A finite element-experimental study of the impact of spheres on aluminium thin plates", *Struct. Eng. Mech.*, **55**(2), 263-280.
Mokhatar, S.N., Sonoda, Y., Kueh, A.B.H. and Jaini, Z.M. (2015), "Quantitative impact response analysis of reinforced concrete beam using the Smoothed Particle Hydrodynamics (SPH) method", *Struct. Eng. Mech.*, **56**(6), 917-938.
Ottosen, N.S. (1977), "A failure criterion for concrete", *J. Eng. Mech.*, ASCE, **103**(4), 527-535.
Pandey, A.K. (2010), "Damage prediction of RC containment shell under impact and blast loading", *Struct. Eng. Mech.*, **36**(6), 729-744.
Riera, J.D. (1968), "On stress analysis of structures subjected to aircraft impact forces", *Nucl. Eng. Des.* **8**(4), 415-426.
Sugano, T., Tsubota, H., Kasai, Y., Koshika, N., Orui, S., von Riesemann, W.A., Bickel, D.C. and Parks, M.B. (1993), "Full-scale aircraft impact test for evaluation of impact force", *Nucl. Eng. Des.*, **140**(3), 373-385.
Thai, D.K. and Kim, S.E. (2015), "Numerical simulation of reinforced concrete slabs under missile impact", *Struct. Eng. Mech.*, **53**(3), 481-495.
Varas, D., Zaera, R. and Lopez-Puente, J. (2009), "Numerical modeling of the hydrodynamic ram phenomenon", *Int. J. Impact Eng.*, **36**(3), 363-374.
Vignjevic, R., De Vuyst, T., Campbell, J. and Libersky, L. (2002), "Modeling of hydrodynamic ram using smoothed particle hydrodynamics", *Proceedings of the Fifth International Conference on Dynamics and Control of Systems and Structures in Space*, Cambridge, UK, July.

PL